Deposition and organisation of cell wall polymers during maturation of poplar tension wood by FTIR microspectroscopy

Shan-Shan Chang, Lennart Salmén, Anne-Mari Olsson, Bruno Clair

Deposition and organisation of cell wall polymers during maturation of poplar tension wood by FTIR microspectroscopy

Shan-Shan Chang · Lennart Salmén · Anne-Mari Olsson · Bruno Clair

Abstract To advance our understanding of the formation of tension wood, we investigated the macromolecular arrangement in cell walls by Fourier transform infrared microspectroscopy (FTIR) during maturation of tension wood in poplar (*Populus tremula* x *P. alba*, clone INRA 717-1B4). The relation between changes in composition and the deposition of the G-layer in tension wood was analysed. Polarised FTIR measurements indicated that in tension wood, already before G-layer formation, a more ordered structure of carbohydrates at an angle more parallel to the fibre axis exists. This was clearly different from the behaviour of opposite wood. With the formation of the S_2 layer in opposite wood and the G-layer in tension wood, the orientation signals from the amorphous carbohydrates like hemicelluloses and pectins were different between opposite wood and tension wood. For tension wood, the orientation for these bands remains the same all along the cell wall maturation process, probably reflecting a continued deposition of xyloglucan or xylan, with an orientation different to that in the S_2 wall throughout the whole process. In tension wood, the lignin was more highly oriented in the S_2 layer than in opposite wood.

Keywords FTIR microscopy · Maturation · Orientation · Polarisation · Polymers · *Populus tremula* x *P. alba* · Tension wood

S.-S. Chang (✉) · B. Clair
Laboratoire de Mécanique et Génie Civil (LMGC),
Université Montpellier 2, CNRS, Pl. E. Bataillon,
cc 048, 34095 Montpellier Cedex 5, France
e-mail: shanshan.chang@univ-montp2.fr;
changelxy@hotmail.com

L. Salmén · A.-M. Olsson
Innventia AB, Drottning Kristinas väg 61, Box 5604,
114 28 Stockholm, Sweden

Abbreviations

CCD	Charge-coupled device
FTIR	Fourier transform infrared
G-layer	Gelatinous layer
I	Intensity absorbance
L	Longitudinal
MCT	Mercury cadmium telluride
OW	Opposite wood
R	Radial
RA	Relative absorbance
ROA	Relative orientation absorbance
S_1	Secondary cell wall layer, first layer
S_2	Secondary cell wall layer, middle layer
S_3	Secondary cell wall layer, third layer
T	Tangential
TW	Tension wood
XET	Xyloglucan-endotransglycosylase

Introduction

In response to changes in environmental factors like slope, winds, snow, or light, trees maintain or reorient their stems and branches by developing reaction wood on one side of the axis (Timell 1986). In angiosperm woody species, this wood, called tension wood, is generally formed on the upper side of the leaning stem and associated with the development of large tensile stresses within the structure (Wardrop 1964; Fisher and Stevenson 1981). In many species, tension wood is characterised by the peculiar longer fibres, called G-fibres, with an inner gelatinous layer, the G-layer. Before fibres reach maturity, the newly divided cells in the vascular cambium pass through four major developmental stages: (i) an increase in cell size (cell elongation and radial enlargement), (ii) secondary

cell wall deposition, (iii) lignification and (iv) cell death. At the beginning of differentiation, the young xylem cells become both longer and wider. At this stage, they only have an ultra-thin primary wall, which comprises cellulose, pectic polysaccharides, xyloglucans and lesser amounts of arabinoxylans and proteins (Cosgrove and Jarvis 2012). Once cell expansion is completed, the secondary cell wall gradually thickens inwards to form a multilayer (S_1, S_2 and S_3) structure comprising cellulose microfibril bundles embedded in an amorphous matrix of hemicelluloses (mainly xylans and glucomannans) and lignin. Cell wall characteristics can be modified during cell maturation by external mechanical stresses, e.g. wind or stem lean, which is the case of G-fibre formation in tension wood in angiosperms. In the G-fibres of tension wood, a thick G-layer may replace the S_3 layer and part of or the whole S_2 layer (Wardrop and Dadswell 1955). This layer is almost free of lignin and consists mainly of highly crystalline cellulose with microfibrils oriented nearly parallel to the fibre axis (Norberg and Meier 1966). Recent analyses indicate that the G-layers in *Populus* also contain some non-cellulosic polysaccharides like xyloglucans and pectin, the two which differ strongly from those in the adjacent secondary (S) layers that mainly contain xylans and glucomannans (Nishikubo et al. 2007; Bowling and Vaughn 2008; Mellerowicz et al. 2008). More recently, Kim and Daniel (2012) also found xylan in the G-layer itself.

The properties of the fibres are mainly determined by the arrangement of the polymers cellulose, hemicelluloses (xylans and glucomannans) and lignin within the cell wall, as well as by interactions among them (Salmén and Burgert 2009). Fourier transform infrared (FTIR) microscopy makes it possible to monitor the development and compositional changes in the cell walls and thus obtain a clearer picture of cell wall development. By using polarised radiation, information on the orientation of specific groups and of the polymer chains containing these groups in the wood structure can be obtained at a μm scale (Olsson et al. 2011). The aim of this study was to better understand how the deposition and organisation of the cell wall polymers relate to tension wood formation by comparing their behaviour to that of opposite wood during wood maturation. FTIR (Fourier transform infrared) microscopy was applied to a sequence of cell differentiation during the formation of the cell wall in poplar tension wood.

Materials and methods

Materials

In vitro shoots of poplar (*Populus tremula* x *P. alba*, clone INRA 717-1B4) were produced at INRA Orleans, France and acclimatised in a greenhouse on the 10th of February 2009. On the 13th of May 2009, the trees were moved outside and artificially tilted at an angle of 35° to the natural curvature to trigger the formation of tension wood, as shown in Fig. 1. Figure 1 also clearly shows that even before tilting, these trees formed tension wood to keep themselves upright. The trees were regularly watered until sampling. About 1 month later (15th of June 2009), the trees were sampled and the samples were frozen and stored until required.

Figure 1 presents the transverse sections of stems stained with safranin/astra blue showing the formation of tension wood after tilting of the stem, represented by the blue-stained G-layers. In the periphery of the stems near the cambium, the newly dividing cells were also stained blue like the G-layer because these cells were not yet lignified and consequently contained relatively more carbohydrate components (cellulose, hemicelluloses and pectin). Sample blocks with a diameter of 20 mm (including differentiating cells) from the upper side of tilted stems from trees marked I and II in the growth season were used. For the sake of comparison, observations were also made on an opposite wood block, but a sample was only taken from the tree marked II because the same section of tree I was too narrow.

Microscopic observations and measurement of cell wall thickness

The wood blocks were dehydrated with ethanol and embedded in LR White resin (two changes of resin/ethanol mixture for 1 h, followed by two exchanges in pure resin for 1 h and kept overnight at room temperature, then polymerised at 65 °C overnight). Transverse sections (1-μm thick) were cut with a diamond knife and observed with an optical microscope (Leica Microsystems) in phase contrast mode. The thickness of the radial cell walls (with and without the G-layer) was measured manually from the raw images using the image analysis software ImageJ (National Institutes of Health, Bethesda, MD, USA).

FTIR measurement

FTIR spectra were recorded in transmission mode on a Spectrum 100 FTIR Spectrometer equipped with a microscope, Spectrum Spotlight 400 FTIR Imaging System (Perkin Elmer). Transverse sections 20-μm thick and successive 20-μm-thick tangential sections (for handling purposes, the tangential sections near the cambium were 30-μm thick to compensate for their low density) from the cambium to full maturation were cut with a vibratome (Leica Microsystems) from both tension and opposite wood blocks. The distance from the cambial zone was recorded for each

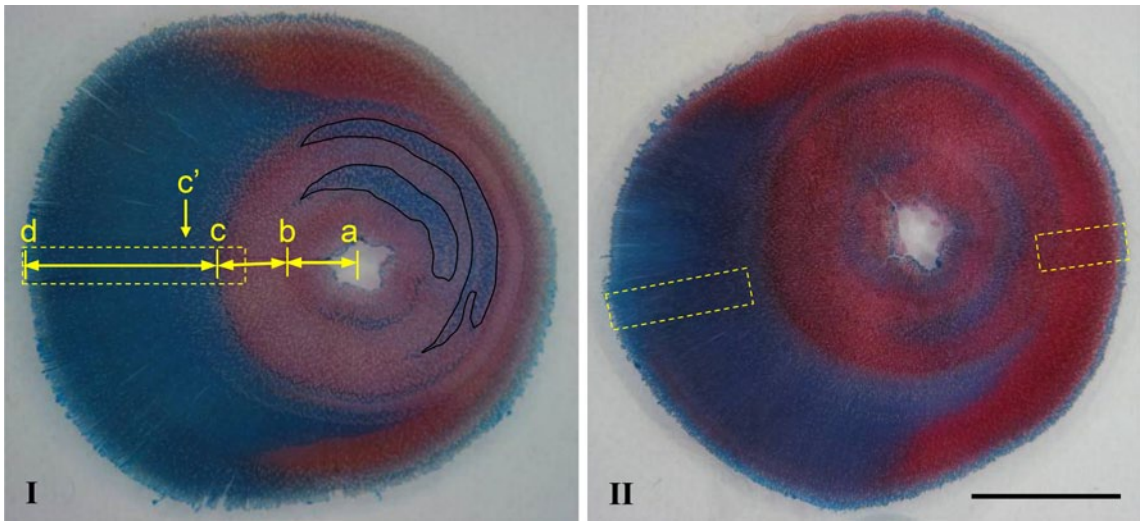

Fig. 1 Light micrograph of transverse section from 1-year-old poplar wood stems stained with safranin/astra blue indicating high concentrations of CH structures, i.e. places where carbohydrate content is high and lignin content is consequently low. Both trees I and II were used for the study of tension wood, but only tree II was used for the study of opposite wood. *a–d* Different growth conditions in tree I: in vitro (*a–b*), grown in the greenhouse (*b–c*), grown outdoors (*c–d*). *a–c* Growth before artificial tilting (unintended tension wood produced on the opposite side; curve regions). *c–d* Growth after tilting at an angle of 35°. *c* Boundary between normal wood and tension wood on the tension wood side. *c′* End of the transition zone. The dotted rectangle indicates the area where FTIR measurements were made. *Scale bar* 5 mm (Images provided by F. Laurans, INRA Orléans, France)

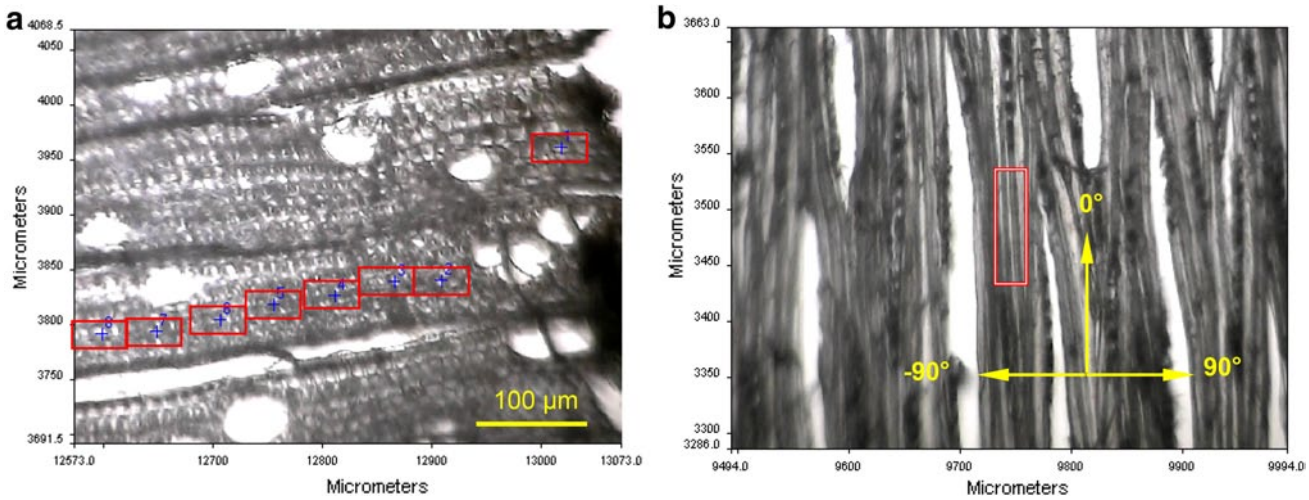

Fig. 2 Visible images of transverse (**a**) and tangential (**b**) sections of poplar tension wood showing the measuring area (a: 50 × 25 µm, R × T; b: 25 × 100 µm, T × L) and the polarization directions of the measurement

tangential section. Air-dried samples were mounted on the autosampler stage which was incorporated in the microscope. The area of interest was first selected from a visible image displayed by a CCD camera and then irradiated with mid-IR light. The transverse microtome sections were then point scanned. Spectra were collected continuously from fibres in small areas of 50 × 25 μm^2 (radial × tangential, R × T) along the radial direction (Fig. 2a). The centre of each measurement area was recorded as the position of each spectrum. One average spectrum was collected from each measuring area.

In each tangential section, a 25 × 100 μm^2 (tangential × longitudinal, T × L) area of fibres (Fig. 2b) was subjected to polarised light by a wire grid polariser from −90° to 90° polarisation in relation to the fibre axis with an interval of 10°. Scanning was performed in imaging mode by an array detector. The detector moved step by step across the preset area until all the spectra had been collected.

For each polariser angle of a given measurement area, 64 different spectra were recorded with a pixel resolution of 6.25 μm × 6.25 μm. The number of spectra collected corresponded to the number of pixels and the preset measuring area. In this way, an IR full-spectral image including spectral information was obtained for each polariser angle of each measuring area. The mean spectrum of the whole image at each polariser angle was used for further data processing. All the spectra discussed above were the average of 16 scans recorded at a resolution of 4 cm^{-1} in the range from 4,000 to 700 cm^{-1} with an MCT detector (cooled in liquid nitrogen).

Data processing

The FTIR spectra were processed using the software Spotlight 1.5.1, HyperView 3.2 and Spectrum 6.2.0 (Perkin Elmer Inc., Shelton, CT, USA). The spectra were corrected by applying an atmospheric correction function to minimise the effects of CO_2 and H_2O. The spectra were baseline corrected at 1,850, 1,540, 1,488, 1,188 and 800 cm^{-1}.

For the spectra acquired with un-polarised light (point mode), the differences in total absorbance due to variations in the thickness of the cell walls of the measured samples were compensated for by normalising the spectra with the total absorbance in the wavenumber range of 1,800–1,140 cm^{-1} (avoiding noise between 1,140 and 800 cm^{-1} due to too high absorbance). The relative absorbance, RA, was calculated as:

$$\mathrm{RA} = I_a/I_t \quad (1)$$

where I_a is the absorbance at a given wavenumber and I_t is the total absorbance in the wavenumber range of 1,800 to 1,140 cm^{-1}.

To compare the orientation spectra, the relative orientation absorbance, ROA, was calculated for each specific absorbance peak as:

$$\mathrm{ROA} = I_p/I\mathrm{max} \quad (2)$$

where I_p is the intensity of the absorbed IR radiation at a given polarisation angle for a specific wavenumber and I_{max} is the maximum intensity in the polarisation interval (−90° to 90°) for the specific wavenumber. A few aberrant points caused by measurement disturbances (e.g., a less flat sample or a sample that became loose during the experiment) were not used in subsequent analyses. As IR absorbance peaks always have some influence from neighbouring peaks, as well as the fact that for small peaks the signal to noise ratio is decreased in these calculations, differences smaller than 0.1 units in peak height in the orientation spectra should be taken with precaution.

IR absorbance of functional groups with vibrations orientated parallel to the fibre axis will have the highest absorbance at low polarisation angles, whereas functional groups oriented perpendicular to the fibre axis will have the highest absorbance at high polarisation angles. Because the IR transmission light will pass through at least two cell walls of adjacent cells (with the middle lamella in between) with opposite fibrillar angles, the oriented molecules will display an average absorption for the two angles, with a peak either at 0° or at 90°. The position depends on whether the main orientation of the molecules is at a lower or higher angle than 45°. The extent of the molecular orientation will instead be noted by the magnitude of the differences in absorbance between polarisation angles. This also implies that molecular groups oriented other than 0 or 90° to the backbone may be difficult to use for orientation assessments.

Results

Change in cell wall thickness

Figures 3a and 4a show variations in the thickness of cell wall layers during maturation of tension wood from tree I and tree II, respectively. The thickness is plotted against the distance from the cambial zone. Figures 3d and 4d are light micrographs of corresponding transverse sections showing cell differentiation from the cambial zone to full maturation.

The gradual thickening of the fibre in the secondary wall layer in tension wood of tree I was clearly visible up to 350 μm from the cambial zone (Fig. 3a; d1–d3 in Fig. 3d). After 350 μm, the G-layers started becoming visible (d4 in Fig. 3d) along with an almost linear increase in the thickness of the G-layer. The thickening of the G-layer was complete in fibres located 900 μm after the cambial zone, after which the cell wall thickness remained constant. The tension wood of tree II showed a similar tendency. The thickness of the G-layer increased linearly from 400 μm until ~900 μm from the cambial zone (Fig. 4a). The sharp increase in the thickness of the G-layer is in agreement with changes in G-layer thickness during fibre differentiation reported by Yoshinaga (Yoshinaga et al. 2012).

Changes in FT-IR spectra

Figure 5 shows a comparison of FTIR spectra at different stages of cell maturation in tension wood of tree I. The selection of the different stages was based on the G-layer formation (Figs. 3a and 4a): before G-layer formation (stage 1, T1), early stage of G-layer formation (stage 2, T2), later stage of G-layer formation (stage 3, T3) and completion of the thickening of the G-layer (stage 4, T4). The main differences in the absorption spectra were visible at

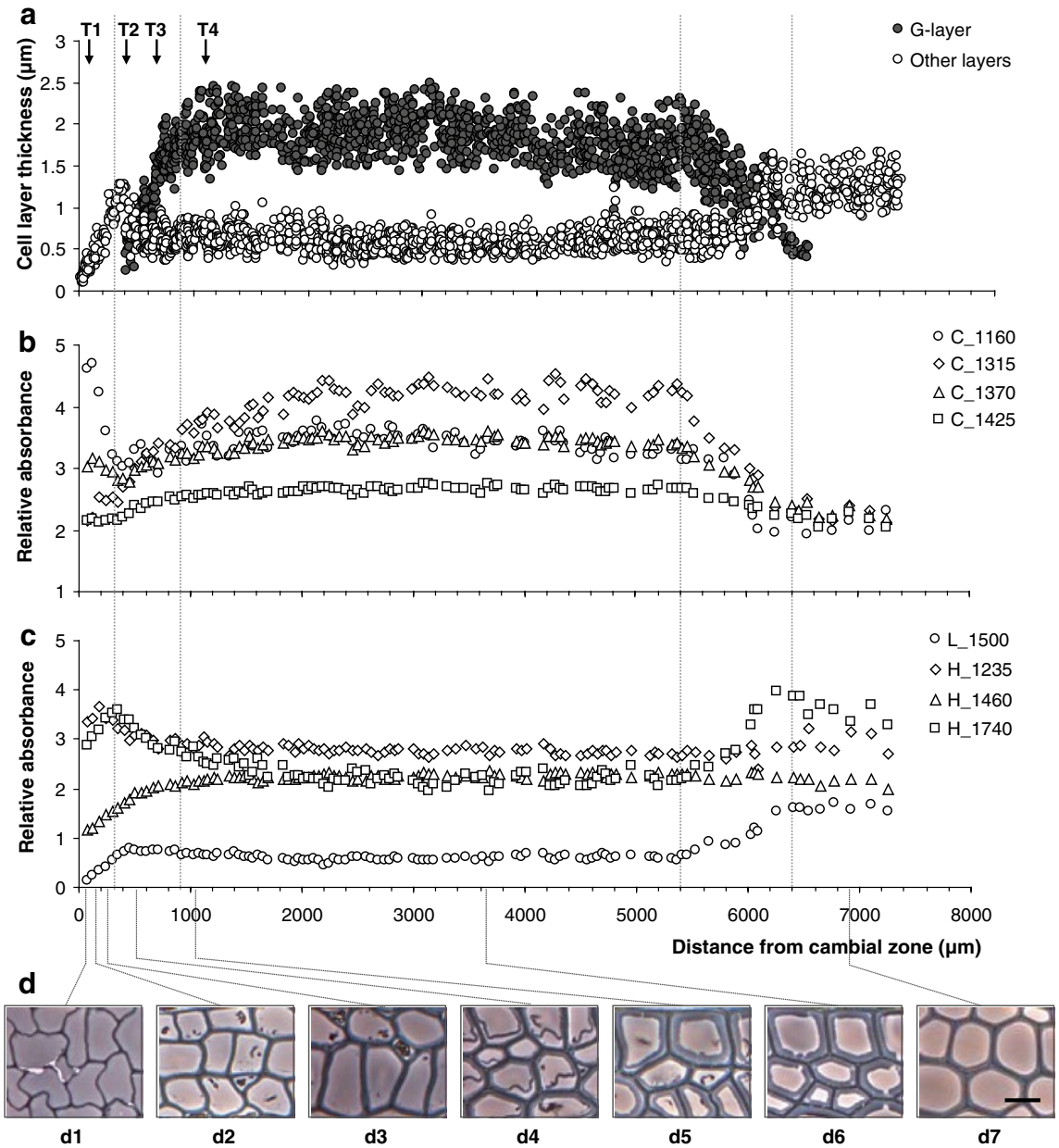

Fig. 3 Changes in cell layer thickness (**a**) and relative intensity of absorbance bands for cellulose and other carbohydrates (**b**), hemicellulose and lignin (**c**) and morphological details of fibre (**d**) during cell wall maturation as well as the annual ring and the normal wood region in poplar tension wood from tree I. *Vertical dotted lines* indicate the different stages of maturation in tension wood. *T1*, *T2*, *T3* and *T4* indicate the four stages of G-layer formation. The light micrographs (*d1–d7*) were collected with an optical microscope in phase contrast mode. At 5,400 µm, the transition from the previously formed normal wood layer is visible. Other layers: sum of all other layers in the cell wall except the G-layer. *Scale bar* (shown in *d7*) = 10 µm

wavenumbers 1,160, 1,235, 1,315, 1,370, 1,425, 1,460, 1,500 and 1,740 cm^{-1}.

Chemical composition

Table 1 lists the typical bands assigned to cellulose, lignin, and xylan (the dominating hemicellulose in hardwood) as well as to pectins and xyloglucans, in the wavenumber interval 1,800–1,100 cm^{-1}. For each assignment of an IR band to a functional group, an interval is given reflecting the range of the maxima reported in the literature.

The relative absorbance of characteristic FTIR absorbance bands is plotted as a function of the stage of maturation of the cell walls in the tension wood of tree I in Fig. 3b, c,

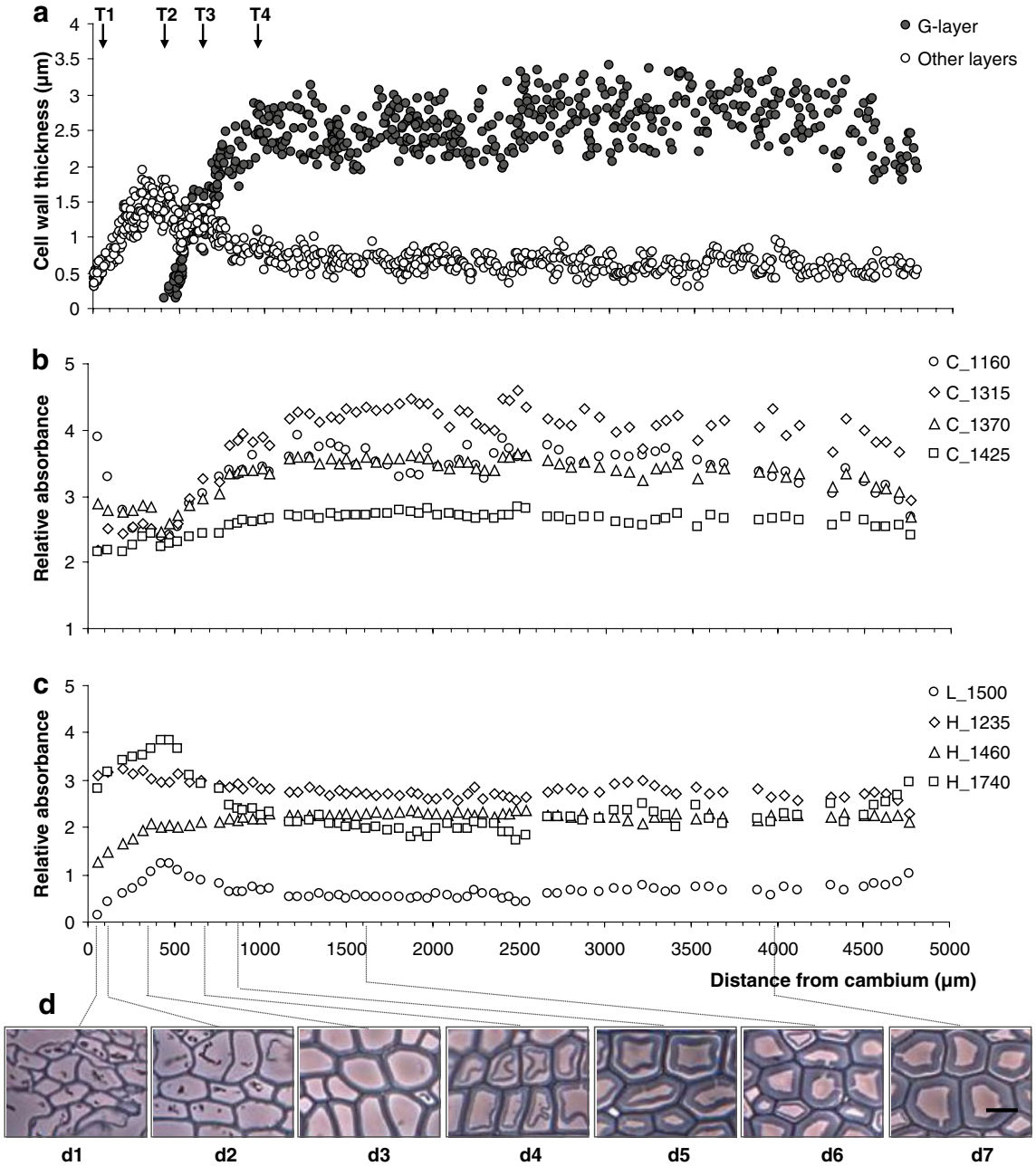

Fig. 4 Changes in cell layer thickness (**a**) and relative intensity of absorbance bands for cellulose and other carbohydrates (**b**), hemicellulose and lignin (**c**) and morphological details of fibre (**d**) during cell wall maturation in poplar tension wood from tree II. *T1*, *T2*, *T3* and *T4* indicate the four stages of G-layer formation. The light micrographs (*d1–d7*) were collected with an optical microscope in phase contrast mode. Other layers: sum of all other layers in cell wall except G-layer. *Scale bar* (shown in *d7*) = 10 µm

and for tree II in Fig. 4b, c. In the tension wood of tree I, early in the cell wall development within the first 350 µm, the absorbance peak of the carbohydrate C–O–C vibration at 1,160 cm^{-1} dominated the spectra. At this stage, the signal can be specifically assigned to cellulose, as indicated by the 1,370 cm^{-1} absorbance peak, and to pectins, as indicated by the large relative sorption peak at 1,740 cm^{-1}, assigned to C=O stretching in the galacturonic acid of pectic substances. At this stage, the discrepancy between the absorbance level of the 1,160 peak and that at 1,315, 1,370 and 1,425 may be due to the high pectin content compared with that of cellulose. Changes in the 1,740 cm^{-1} peak were at this stage also influenced by the deposition of xylan. With lignification, absorbance increased at 1,500 cm^{-1} and the

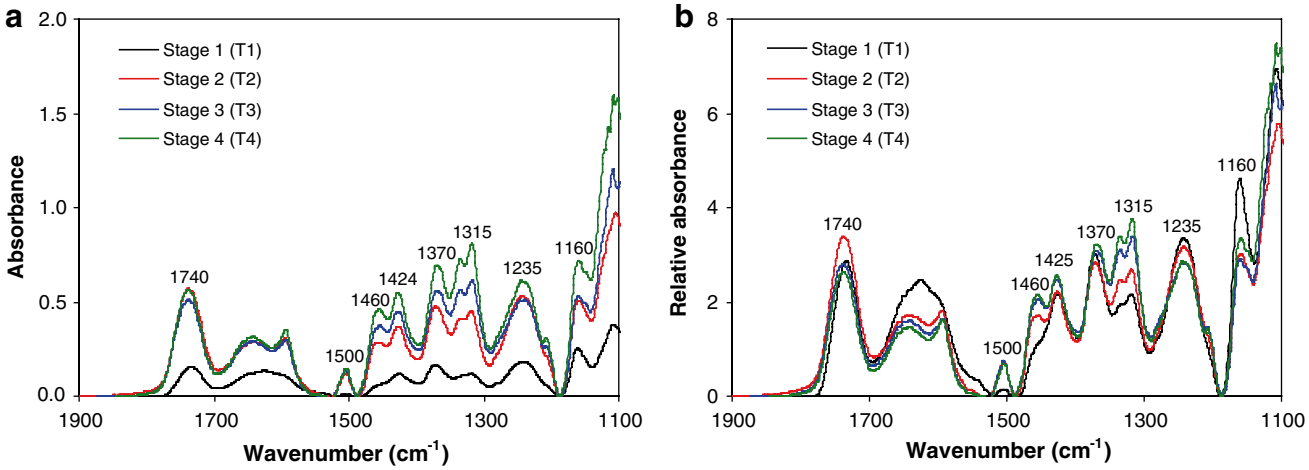

Fig. 5 Non-polarised FTIR spectra in the region from 1,800 to 1,100 cm^{-1} at four stages *(T1, T2, T3, T4)* of cell wall differentiation in poplar tension wood from tree I. **a** Non-normalized spectra; **b** normalized spectra. The *peak numbers* refer to the assignments in Table 1

Table 1 Assignment of IR bands in the range of 1,800–1,100 cm^{-1} to functional groups of wood polymers

Wavenumber (cm^{-1}) range of maxima	Assignment	Orientation of polarisation to main axis of polymer	Components
1,158–1,162	C–O–C asymmetric stretch	0°	Dominated by cellulose (Liang and Marchessault 1959; Liang et al. 1960; Marchessault 1962), but present in all carbohydrates
1,232–1,239	C–O stretching in O=C–C group	90°	Xylan, lignin–carbohydrate complex (Marchessault 1962)
1,312–1,316	CH_2 wagging	90°	Cellulose (Liang and Marchessault 1959)
1,365–1,372	C–H bending	0°	Cellulose (crystalline) (Liang and Marchessault 1959; Marchessault 1962)
1,421–1,430	C–OH bending of the CH_2–OH group	0°	Cellulose (Marchessault 1962)
1,452–1,462	CH_2 symmetric bending on xylose ring	90° (0° to glucan chain in xyloglucan)	Xylan (Marchessault 1962), Xyloglucan (Vodenicarova et al. 2006)
	CH deformation in CH_3 and CH_2	–	Lignin (Faix 1991)
1,500–1,510	C=C aromatic symmetrical stretching	0°	Lignin (Marchessault 1962; Faix 1991)
1,730–1,742	C=O stretching in glucuronic acid	54°	Xylan (Marchessault 1962; Marchessault and Liang 1962)
	C=O stretching in galacturonic acid/acetyl esters	?	Pectins (Synytsya et al. 2003; Fellah et al. 2009)

relative absorbance peaks associated with carbohydrates generally diminished except for the 1,460 cm^{-1} band related to xylan deposition which occurred at the same time. This band shows also contribution from lignin vibrations, but is more strongly influenced by molecular vibrations of the xylose unit (Stevanic and Salmén 2009). The decrease was especially apparent in the 1,740 cm^{-1} band and could be associated with a drop in relative pectin content. With the formation of the G-layer, identified by the change in cell wall thickness (Fig. 3a) and by microscope observations (d4–d5 in Fig. 3d), relative cellulose content increased (the relative increase in the absorbance peaks at 1,315, 1,370 and 1,425 cm^{-1}). At the same time, a further increase in the relative absorbance peak of the 1,460 cm^{-1} band was visible. This was probably due to the deposition of xyloglucans. After completion of G-layer formation in the interval from 900 to 5,400 μm from the cambial zone, the relative intensity of each band remained constant until the transition, between 5,400 and 6,400 μm (c′–c in Fig. 1) to normal wood (c–b in Fig. 1). The light micrographs of the transverse sections (Fig. 1) did not show the presence of a G-layer in this region, which was created before the tilting of the stem and

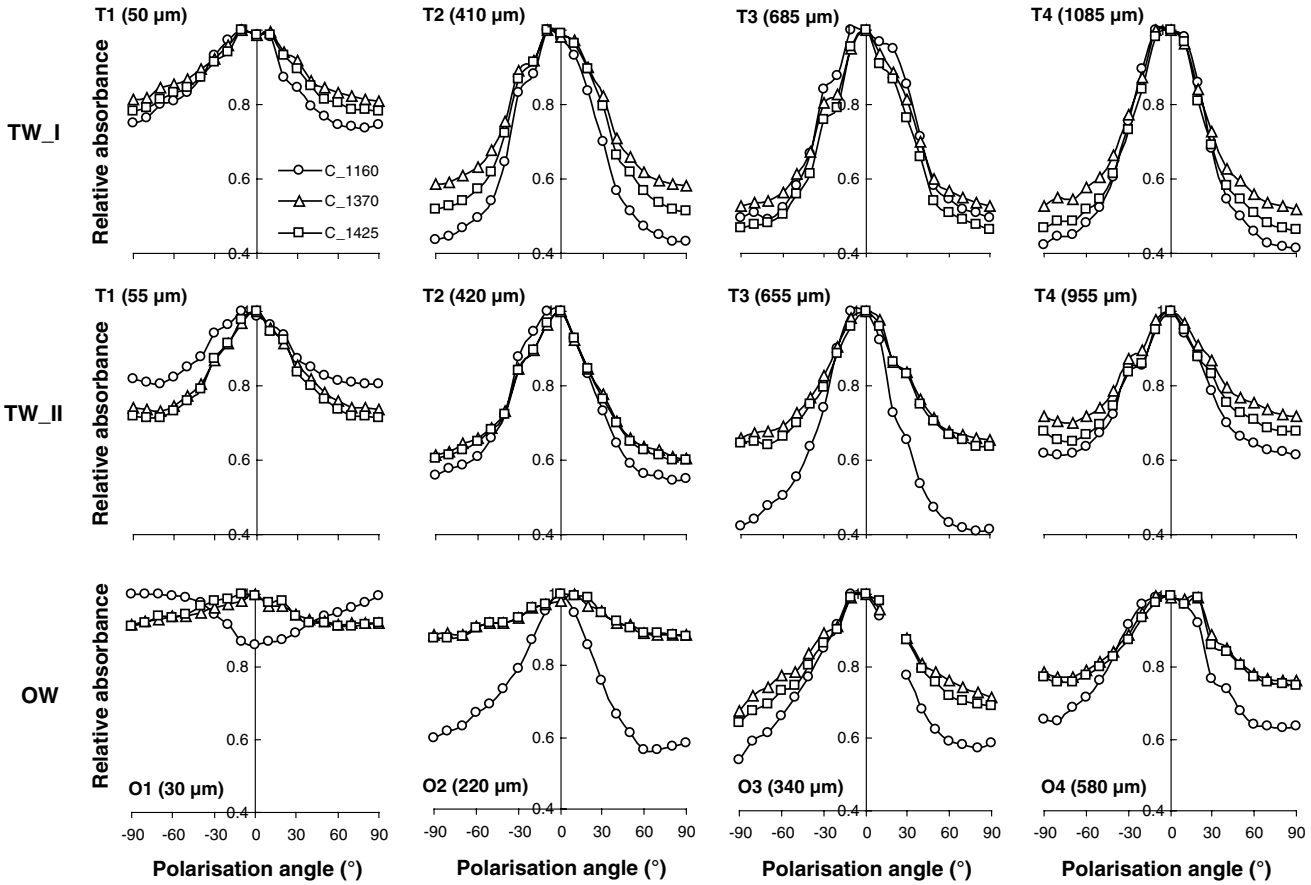

Fig. 6 Orientation distribution of typical bands assigned to cellulose for spectra taken from four stages (*T1/O1*, *T2/O2*, *T3/O3*, *T4/O4*) during cell differentiation of poplar tension (TW) and opposite wood (OW) (*TW_I* and *TW_II* denote tension wood taken from tree I and II, respectively; the distance from the cambium zone is given in brackets; a few aberrant points due to measurement disturbances were removed from the figure)

consequently contained relatively less cellulose and more lignin and hemicellulose than tension wood. The tension wood of tree II revealed similar changes in band intensities during maturation of the cell wall (Fig. 4b, c). However, measurements were not made right up to the stage of the normal wood before tilting.

Concerning opposite wood, it was not possible to monitor the early part of the cell wall formation with FTIR measurements. After formation of the final secondary cell wall, the relative intensities of the IR absorbance bands were constant, as observed in the normal wood region in the tension wood side (data not shown).

Molecular orientation

Figures 6, 7 and 8 compare the molecular orientation assigned to cellulose, lignin, and hemicelluloses and pectins at four stages during cell differentiation of tension and opposite wood from tree I and tree II, respectively. For tension wood, the selection of the four stages was the same as for FTIR spectra comparison (Fig. 5). For opposite wood, the stages were defined as: O1, early stage of cell wall thickening; O2, later stage of cell wall thickening; O3, completion of cell wall thickening and O4, the mature cell wall.

Figure 6 presents diagrams of the orientation of the absorbance peaks assigned primarily to cellulose. For tension wood, no apparent changes were observed as a function of the stages of cell maturation and the fibrillar orientation was in all cases parallel to the fibrillar axis; i.e. to the fibre axis considering that the microfibril angle is generally low for these fibres. As G-layer formation proceeded, the amount of highly orientated cellulose increased, following the completion of thickening of the G-layer, as indicated by the increased difference in absorbance between polarisation angles. For the opposite wood, at the early stage of cell wall thickening, indications of orientation are rather small, if any; a small orientation of the 1,160 cm^{-1} band perpendicular (90°) to the fibre axis was noted (absorbance differences between 1.0 and 0.9 may be too low to indicate

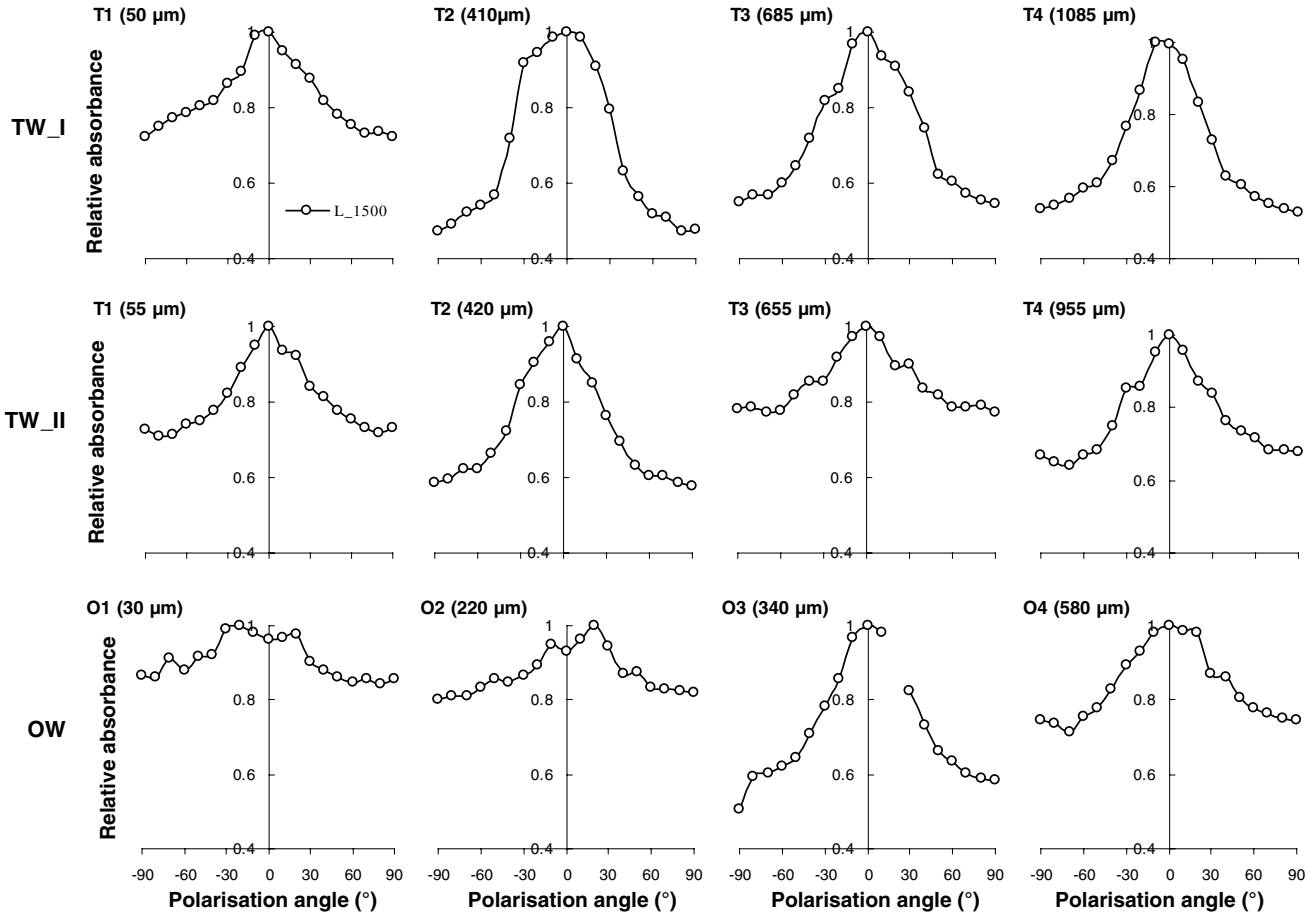

Fig. 7 Orientation distribution of the absorption band assigned to lignin for spectra taken from four stages (*T1/O1*, *T2/O2*, *T3/O3*, *T4/O4*) of cell differentiation of poplar tension (TW) and opposite wood (OW) (*TW_I* and *TW_II* denote tension wood taken from tree I and II, respectively; the distance from the cambium zone is given in brackets; a few aberrant points due to measurement disturbances were removed from the figure)

orientation). At this stage, microscope observation only indicated the presence of the primary wall and/or S_1 layer, while the S_2 layer was subsequently formed and thickened when the distance from the cambial zone was greater than 60 µm. At this stage, the C–O–C orientation probably may reflect a perpendicular orientation of cellulose in the primary wall, S_1 layer. However, it should be noted that the C–O–C absorption peak at 1,160 cm^{-1} also has contributions from all carbohydrates present and the discrepancy in the orientation of the peaks at 1,370 and 1,425 cm^{-1} may point to orientation contribution in these layers, the primary and S_1 layer, from other carbohydrates. At later stages of cell wall formation, when the S_2 layer was laid down, the difference in absorbance between polarisation angles indicated a smaller proportion of cellulose oriented at an angle of 0° than that observed in tension wood. Compared with tension wood, the orientation distributions for bands assigned to cellulose in opposite wood generally had wider peaks, especially the bands at 1,370 and 1,425 cm^{-1}. This probably reflects the fact that, unlike in tension wood, in opposite wood, absorbance was not dominated by the thick G-layer but showed a mix of contributions from the orientations of microfibrils in the S_1, S_2 and S_3 layer.

The absorbance peak at 1,500 cm^{-1}, assigned to lignin (Fig. 7), showed a surprisingly high degree of orientation compared to that observed for cellulose (only slightly lower in magnitude between the differences in absorbance between polarisation angles; Fig. 6) both for tension wood and opposite wood. This orientation of lignin has also previously been demonstrated by Raman spectroscopy (Agarwal and Atalla 1986) in the transverse plane and by FTIR in the longitudinal direction (Salmén et al. 2012). In all cases, the peak was clearly centred around 0°, indicating that lignin was oriented more or less parallel to the fibre axis except during the early stages of cell maturation in opposite wood. In tension wood, oriented lignin was observed early in the cell wall development at low lignin content and before G-layer deposition. As the formation of the G-layer

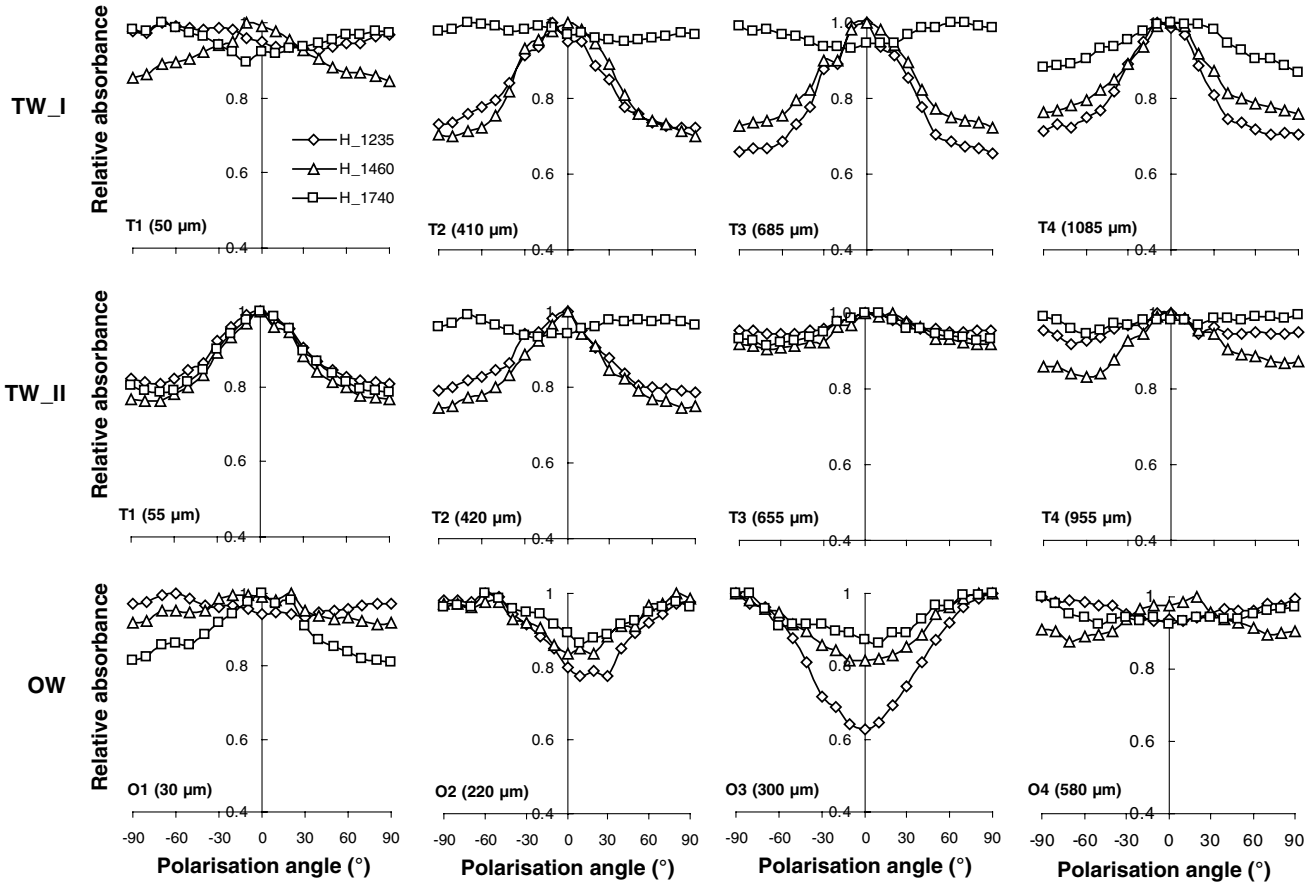

Fig. 8 Orientation distribution of typical bands assigned to carbohydrates like hemicelluloses and pectins for spectra taken from four stages (*T1/O1*, *T2/O2*, *T3/O3*, *T4/O4*) during cell differentiation in poplar tension (TW) and opposite wood (OW) (*TW_I* and *TW_II* denote tension wood taken from tree I and II, respectively; the distance from the cambium zone is shown in brackets)

advanced, the degree of orientation increased and became more distinct at the later stage of G-layer formation. Opposite wood generally showed a higher relative absorbance for the lignin peak at 1,500 cm^{-1}, reflecting the higher overall lignin content compared to tension wood. The lignin present in tension wood is mostly associated with the S_2 wall and the lignin content in the G-layer is low or even nil (Pilate et al. 2004). In the present study, the difference in absorbance between polarisation angles was however generally found to be lower in opposite wood than in tension wood (Fig. 7).

Figure 8 shows the orientation dependence of peaks assigned to hemicelluloses and pectin. At 1,235 and 1,460 cm^{-1}, vibrations are traditionally thought to be dominated by the C–O stretching in the O=C–O group of xylans and the CH_2 asymmetric bending of the xylose ring, respectively. Both are assigned as being perpendicular to the main chain axis (Marchessault 1962). During the formation of the G-layer in tension wood, these two absorbance signals showed clear orientation dependence, with higher absorbance at lower polarisation angels; i.e. at an angle of 0°. This implies an orientation of the structure of xylose units of the carbohydrates at an angle of 90° to that of the cellulose, a fact that has also previously been observed and related to the presence of xyloglucans oriented parallel to the cellulose in the same direction as the fibre axis (Olsson et al. 2011) (the xylose units of xyloglucan being oriented perpendicular to the glucan backbone). It should be noted that a difference in absorbance between 1.0 and 0.9 with polarisation angle may not be taken as an indication of orientation due to the normal variation in this type of measurements. Also in the early stage, T1, of cell differentiation in tension wood, the orientation of the CH_2 1,460 cm^{-1} peak was similar to that in the later stage.

In the early stage of cell differentiation, the vibration at 1,740 cm^{-1} was assigned to C=O stretching in galacturonic acid of pectic substances. In the later stage of secondary cell wall thickening, the band at 1,740 cm^{-1} was assigned to C=O stretching in glucuronic acid of xylan. This vibration is predominately oriented at an angle of 54° to the xylose unit of the xylan backbone in hardwood (Marchessault and Liang 1962) which is why little information may

be gained regarding orientation from this absorbance peak, as discussed earlier. In opposite wood, at a later stage of cell wall thickening (stage 2, O2) and the stage of completion of cell wall thickening (stage 3, O3), the peaks at 1,235, 1,460 and 1,740 cm^{-1} in general had a maximum relative absorbance at high angles. This is in agreement with earlier findings, suggesting the orientation of xylan parallel to that of the cellulose microfibrils (Marchessault and Liang 1962; Olsson et al. 2011).

Before the deposition of the G-layer in tension wood, the hemicellulose signals at 1,235, 1,460 and 1,740 cm^{-1} showed similar orientations both in tension and opposite wood. In the following stages of G-layer formation, the orientation of the signals in tension wood remained the same, while in opposite wood the orientation of the signals at the stage of secondary cell wall thickening changed and was opposite to that in tension wood.

Discussion

In cells at the early stage of cell wall thickening (Stage 1, O1) in opposite wood, which only contained primary wall/S_1 wall, a perpendicular (90°) orientation of the cellulose 1,160 cm^{-1} peak was observed. In the following cell wall thickening stages when the S_2 wall dominated, the cellulose showed a more parallel (0°) orientation. This is in agreement with general microscope observations of cellulose microfibril orientation and with results of studies of changes in cellulose structure during maturation by Kataoka and Kondo (1998). The orientation of the primary wall cellulose is directly related to the enlarging cells, resulting in a less orientated distribution than that in the mature wood cell wall. However, in tension wood, an orientation parallel to the fibre axis was already visible at the early stage of cell wall development. This orientation was less clear than that of cells with full S_2 wall formation, but nevertheless distinct. This is surprising considering the rather low cellulose content compared to other carbohydrates. The more distinct orientation of the lignin at this stage also indicates a more ordered cell wall formation and a difference in the structure of tension wood to that of opposite wood already at this stage of cell wall maturation.

Although small amounts of lignin-like compounds have been detected in the G-layer of some tension wood fibres (Joseleau et al. 2004; Gierlinger and Schwanninger 2006), we conclude that most of the lignin signal originates from the lignified S_2 layer and very little from the G-layer (given the marked difference in lignin content between the G-layer and the adjacent S_2 layer and also the fact the G-layer is thicker). The orientation distribution of lignin was more or less parallel to the fibre axis, which was in line with earlier observations in hybrid aspen (Olsson et al. 2011). However, it should be noted that, compared to opposite wood, the higher degree of orientation of the lignin found in tension wood probably implies a higher degree of ordering and orientation of the secondary wall in tension wood fibres than in the corresponding S_2 wall of opposite wood.

In the case of hemicelluloses and pectins, different orientations were observed between tension and opposite wood during formation of the G-layer. Although the mechanism behind the generation of stress in tension wood remains unknown, the matrix polysaccharides in the G-layer probably undergo mechanical stress due to chemical reactions and interaction with the cellulose microfibrils (Mellerowicz et al. 2008) which could result in increased orientation of the polymers. It is also possible that at this stage of development, other polysaccharides like xyloglucan or pectins in the G-layer (Nishikubo et al. 2007; Bowling and Vaughn 2008; Mellerowicz et al. 2008; Kaku et al. 2009; Mellerowicz and Gorshkova 2012) may dominate the signals, as has been suggested in aspen tension wood (Olsson et al. 2011). The tensional stress in the G-layer can only be transmitted to adjacent layers when these are connected by xyloglucan cross-links or long-lived xyloglucan-endo-transglycosylase (XET) activity (Mellerowicz et al. 2008). However, some of the signals may also be related to xylan as it was recently reported that the G-layer may also contain xylan (Kim and Daniel 2012). The question remains, however, why, if so, this xylan is organised perpendicular to the orientation seen in opposite wood.

Conclusion

Polarised FTIR measurements revealed that in tension wood, at the early stage of cell wall development already before the formation of the G-layer, the C–O–C adsorption peak from carbohydrates showed an orientation more parallel to the fibre axis. This behaviour clearly differed from that in opposite wood. In the later stages of G-layer formation, a higher degree of orientation of cellulose was observed in tension wood than in opposite wood. In all cases, the orientation of lignin was parallel to that of cellulose microfibrils, with a higher degree of orientation in tension wood than in opposite wood. This is attributed to a more ordered S_2 wall in tension wood than in opposite wood. During the formation of the G-layer in tension wood, signals attributed to amorphous carbohydrates (hemicelluloses and pectins) were oriented at an angle of 90° to that measured in opposite wood. These signals may originate from the generation of xyloglucan regulating stress in *Populus* tension wood (Baba et al. 2009), but could also be attributed to xylan (Kim and Daniel 2012). In tension wood, the orientation of the bands assigned to amorphous carbohydrates remained the same throughout the cell wall

maturation process, probably reflecting continued deposition of xyloglucan or of xylan with a different orientation from that in the S_2 wall of opposite wood.

Acknowledgments This work was supported by COST Action FP0802 through the Short Term Scientific Mission (STSM) funding for Shan Shan Chang. Shan Shan Chang benefits a fellowship from the Scientific Council of Montpellier University. Lennart Salmén received support from the Wallenberg Wood Science Center (WWSC). The authors wish to thank Gilles Pilate and Françoise Laurans (AGPF, Genobois technical platform, INRA Orleans, France) for providing the wood samples and for making the stained sections presented in Fig. 1, Jasna Stevanic Srndovic and Joanna Hornatowska (Innventia Stockholm, Sweden) for their assistance during FTIR experiment. Thanks are also extended to Cécile Barron (INRA Montpellier, France) and Antonio Pizzi (ENSTIB-LERMAB Epinal, France) for critical discussions. Part of this work was performed in the framework of the project "StressInTrees" funded by the French National Research Agency (ANR-12-BS09-0004).

References

Agarwal UP, Atalla RH (1986) In-situ Raman microprobe studies of plant cell walls: macromolecular organization and compositional variability in the secondary wall of *Picea mariana* (Mill.) B.S.P. Planta 169:325–332

Baba K, Park YW, Kaku T, Kaida R, Takeuchi M, Yoshida M, Hosoo Y, Ojio Y, Okuyama T, Taniguchi T, Ohmiya Y, Kondo T, Shani Z, Shoseyov O, Awano T, Serada S, Norioka N, Norioka S, Hayashi T (2009) Xyloglucan for generating tensile stress to bend tree stem. Mol Plant 2:893–903

Bowling AJ, Vaughn KC (2008) Immunocytochemical characterization of tension wood: gelatinous fibers contain more than just cellulose. Am J Bot 95:655–663

Cosgrove DJ, Jarvis MC (2012) Comparative structure and biomechanics of plant primary and secondary cell walls. Front Plant Sci 3:204. doi:10.3389/fpls.2012.00204

Faix O (1991) Classification of lignins from different botanical origins by FTIR spectroscopy. Holzforschung 45:21–27

Fellah A, Anjukandi P, Waterland MR, Williams MAK (2009) Determining the degree of methylesterification of pectin by ATR/FT-IR: methodology optimisation and comparison with theoretical calculations. Carbohydr Polym 78:847–853

Fisher JB, Stevenson JW (1981) Occurence of reaction wood in branches of dicotyledons and its role in tree architecture. Bot Gaz 142:82–95

Gierlinger N, Schwanninger M (2006) Chemical imaging of poplar wood cell walls by confocal Raman microscopy. Plant Physiol 140:1246–1254

Joseleau JP, Imai T, Kuroda K, Ruel K (2004) Detection in situ and characterization of lignin in the G-layer of tension wood fibres of *Populus deltoids*. Planta 219:338–345

Kaku T, Serada S, Baba K, Tanaka F, Hayashi T (2009) Proteomic analysis of the G-layer in poplar tension wood. J Wood Sci 55:250–257

Kataoka Y, Kondo T (1998) FT-IR microscopic analysis of changing cellulose crystalline structure during wood cell wall formation. Macromolecules 31:760–764

Kim JS, Daniel G (2012) Distribution of glucomannans and xylans in poplar xylem and their changes under tension stress. Planta 236:35–50

Liang CY, Marchessault RH (1959) Infrared spectra of crystalline polysaccharides II. Native celluloses in the region from 640–1,700 cm^{-1}. J Polym Sci 39:269–278

Liang CY, Bassett KH, McGinnes EA, Marchessault RH (1960) Infrared spectra of crystalline polysaccharides. Tappi J 43:1017–1024

Marchessault RH (1962) Application of infra-red spectroscopy to cellulose and wood polysaccharides. Pure Appl Chem 5:107–129

Marchessault RH, Liang CY (1962) The infrared spectra of crystalline polysaccharides VIII. Xylans. J Polym Sci Pol Chem 59:357–378

Mellerowicz EJ, Gorshkova TA (2012) Tensional stress generation in gelatinous fibres: a review and possible mechanism based on cell-wall structure and composition. J Exp Bot 63:551–565

Mellerowicz EJ, Immerzeel P, Hayashi T (2008) Xyloglucan: the molecular muscle of trees. Ann Bot-London 102:659–665

Nishikubo N, Awano T, Banasiak A, Bourquin V, Ibatullin F, Funada R, Brumer H, Teeri T, Hayashi T, Sundberg B, Mellerowicz EJ (2007) Xyloglucan endotransglycosylase (XET) functions in gelatinous layers of tension wood fibers in poplar: a glimpse into the mechanism of the balancing act of trees. Plant Cell Physiol 48:843–855

Norberg PH, Meier H (1966) Physical and chemical properties of gelatinous layer in tension wood fibers of aspen (*Populus tremula* L.). Holzforschung 20:174–178

Olsson AM, Bjurhager I, Gerber L, Sundberg B, Salmén L (2011) Ultra-structural organization of cell wall polymers in normal and tension wood of aspen revealed by polarization FTIR microspectroscopy. Planta 233:1277–1286

Pilate G, Chabbert B, Cathala B, Yoshinaga A, Leplé JC, Laurans F, Lapierre C, Ruel K (2004) Lignification and tension wood. C R Biol 327:889–901

Salmén L, Burgert I (2009) Cell wall features with regard to mechanical performance COST Action E35: wood machining–micromechanics and fracture. Holzforschung 63:121–129

Salmén L, Olsson A-M, Stevanic J, Simonović J, Radotić K (2012) Structural organisation of the wood polymers in the wood fibre structure. Bioresources 7:521–532

Stevanic J, Salmén L (2009) Orientation of the wood polymers in the cell wall of spruce wood fibres. Holzforschung 63:497–503

Synytsya A, Copikova J, Matejka P, Machovic V (2003) Fourier transform Raman and infrared spectroscopy of pectins. Carbohydr Polym 54:97–106

Timell TE (1986) Compression wood in gymnosperms. Springer, Heidelberg

Vodenicarova M, Drimalova G, Hromadkova Z, Malovikova A, Ebringerova A (2006) Xyloglucan degradation using different radiation sources: a comparative study. Ultrasonics Sonochem 13:157–164

Wardrop AB (1964) The reaction anatomy of arborescent angiosperms. In: Zimmermann MH (ed) The formation of wood in forest tree. Academic Press, New York, pp 405–456

Wardrop AB, Dadswell HE (1955) The nature of reaction wood IV. Variations in cell wall organization of tension wood fibres. Aust J Bot 3:177–189

Yoshinaga A, Kusumoto H, Laurans F, Pilate G, Takabe K (2012) Lignification in poplar tension wood lignified cell wall layers. Tree Physiol 32:1129–1136